Neuron
Previews

Macrocircuits for Sound Localization Use Leaky Coincidence Detectors and Specialized Synapses

Christine V. Portfors[1,*] and Henrique von Gersdorff[2,*]
[1]Washington State University, Vancouver, WA 98686, USA
[2]Vollum Institute, Oregon Health and Science University, Portland, OR 97239, USA
*Correspondence: portfors@vancouver.wsu.edu (C.V.P.), vongersd@ohsu.edu (H.v.G.)
http://dx.doi.org/10.1016/j.neuron.2013.05.034

The auditory system computes sound location by detecting submillisecond time differences in the arrival of sound at the two ears. Studies by van der Heijden et al. (2013) and Roberts et al. (2013) in this issue of *Neuron* shed light on how this is accomplished by the interaction of excitatory and inhibitory synapses.

Localizing sound sources is vital for the survival of predators, or to escape from them. Consequently, the auditory system has evolved macrocircuits and specialized synapses that precisely calculate the locus of sound sources (Figure 1A; Ashida and Carr, 2011). The barn owl exemplifies an animal that has exquisite sound localization ability. Barn owls can determine the location of a mouse in absolute darkness with a resolution of less than one degree (Payne, 1971). Because of this amazing accuracy, the barn owl has been a model system for understanding neural mechanisms of sound localization. Humans can also determine the location of a sound with high resolution (e.g., 1–2 degrees; Grothe et al., 2010). Understanding the neural mechanisms underlying this level of accuracy has been of considerable interest for many decades. Two papers in this issue of *Neuron* (van der Heijden et al., 2013, and Roberts et al., 2013) now provide new insights into the mechanisms of mammalian sound localization.

In contrast to other sensory systems, such as vision and somatosensation, the sensory epithelium of the inner ear does not have an explicit representation of space. The inner hair cells are systematically arranged along the basilar membrane to create a place-code for sound frequency but not a code for auditory space. Consequently, the location of a sound source in space must be computed by the auditory system. There are two binaural cues that can be utilized to locate sounds in the horizontal plane; interaural timing differences (ITDs) and interaural level differences (ILDs). ITDs are employed in low-frequency (<2 kHz) localization tasks, and ILDs are employed in high-frequency localization tasks. When the wavelength of a sound is roughly equal to or shorter than the diameter of the head, an ILD is created because of a shadowing effect at the ear further from the sound source. Many mammals, including humans and cats, make use of both ITDs and ILDs for horizontal sound localization whereas some animals such as bats, only use ILD because of their small head size and dependence on hearing ultra high frequency (e.g., 60–120 kHz) sounds for echolocation behaviors. Surprisingly, Mongolian gerbils use ITDs even with their relatively small head (Heffner and Heffner, 1988). This is thought to be because gerbils have a need for long distance communication and thus have evolved low-frequency hearing and use of low-frequency vocalizations. As a result, cats and gerbils have been the animals of choice for understanding mechanisms of ITD coding, whereas many studies have used bats to understand mechanisms of ILD coding.

When sound sources are off the midsagittal plane, they generate differences in the arrival time of the stimulus at the two ears (onset ITD; Figure 1B) and throughout the duration of the stimulus (ongoing ITD). Even at the most extreme horizontal sound position, the ITDs are extremely small; 700 μs in humans, 400 μs in cats, and 135 μs in gerbils (Figure 1B). Amazingly, however, humans can discriminate ITDs of 10–20 μs for low-frequency sounds, and they are capable of discriminating ILDs of 1–2 dB (Grothe et al., 2010). While discrimination ability for both ITDs and ILDs is impressive, the submillisecond resolution of the ITD cue is hard to comprehend considering the millisecond duration of action potentials in the auditory nerve. Thus, there has been considerable interest in the neural and biophysical mechanisms that support this exquisite temporal processing.

In mammals, the extraction of timing cues is performed by bipolar neurons in the medial superior olive (MSO). MSO neurons receive bilateral excitatory input from spherical bushy cells in the cochlear nucleus (Figure 1A). Ipsilateral inputs synapse onto lateral dendrites and contralateral inputs synapse onto the medial dendrites (Figure 1A). Remarkably, these inputs are phase-locked to the stimulus waveform with a precision even greater than that observed in auditory nerve fibers, due to the fast synaptic inputs from the endbulb of Held synapses onto spherical bushy cells (Figure 1C). MSO neurons also show phase-locked responses to monaural stimulation; however, binaural stimulation at a best ITD generates a response that is greater than the sum of the monaural responses (Figure 1D; Joris et al., 1998) and has a higher degree of phase-locking than at unfavorable ITDs (Yin and Chan, 1990). Thus, MSO neurons show submillisecond selectivity to ITDs. Note that the peak and the slope of the ITD function can be used to encode the location of the sound in cats (blue rectangle in Figure 1D), whereas the peak ITD for gerbils may lie outside of the physiologically relevant time range (Grothe et al., 2010). Thus, there may be differences in the ITD coding mechanisms in cats and the small-headed gerbil.

A simple, but seminal model to describe coding of ITD was proposed by Jeffress in 1948. According to this model, coincidence detectors receive

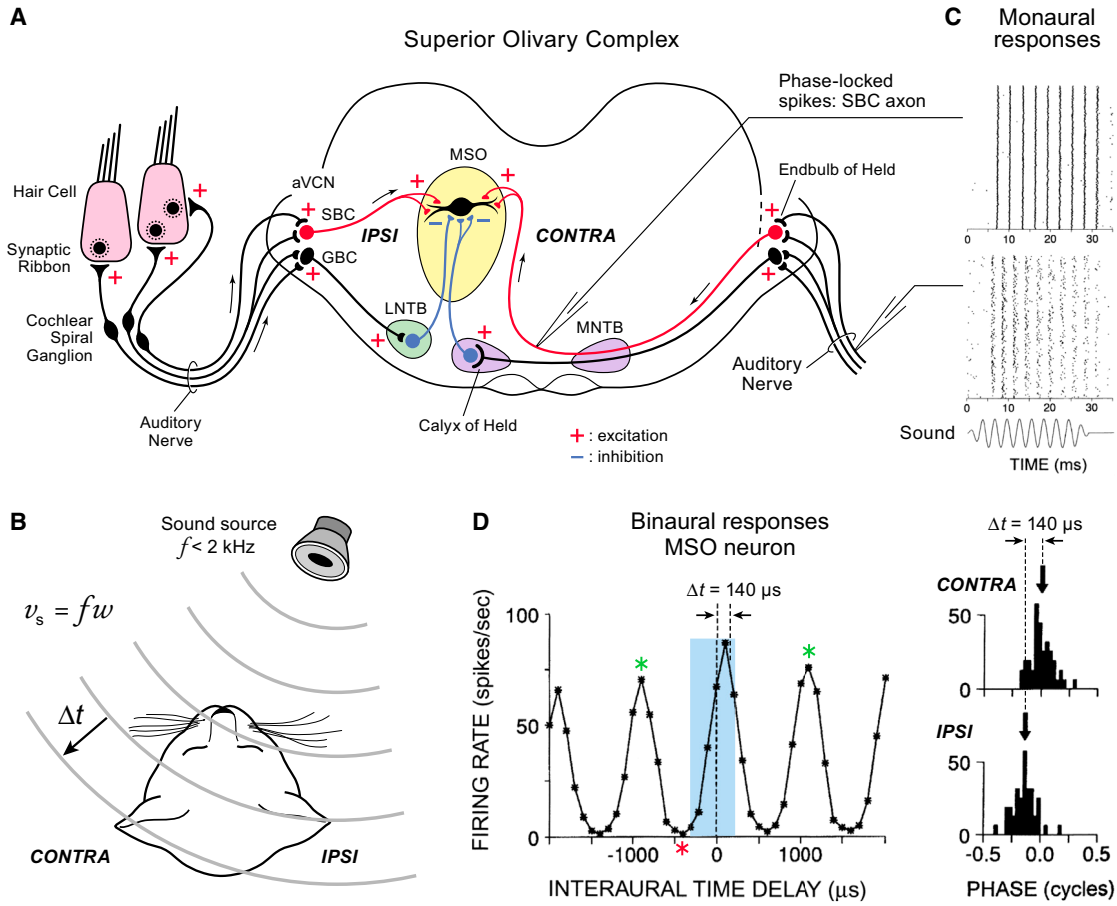

Figure 1. The Mammalian Macrocircuit for the Localization of Low-Frequency Sounds

(A) Sound-evoked signals are detected by inner hair cells in the cochlea and transmitted by specialized ribbon-type synapses to the afferent fibers (or dendrites) of spiral ganglion cells whose axons form the auditory nerve. Some of these axons terminate in the anterior ventral cochlear nucleus (aVCN) where they synapse onto spherical bushy cells (SBC), via large endbulbs of Held, and onto globular bushy cells (GBC). The ipsilateral axons of the spherical bushy cells then form excitatory synapses on the principal cells of the medial superior olive (MSO), which also receive inputs from the contralateral SBC. The MSO principal cell integrates the two excitatory inputs that originate from the two ears. They are thus coincidence detectors of binaural signals. The superior olivary complex also has two nuclei (the lateral and medial nucleus of the trapezoid body: LNTB and MNTB) that send inhibitory input to the MSO. This inhibitory input can arrive before the excitatory input and thus can shape the response of the MSO cells.

(B) Low-frequency sounds that are located at an angle to the midsagittal plane arrive in the ipsilateral (*IPSI*) ear before they reach the contralateral ear (*CONTRA*). Given the constant speed of sound ($v_s = f\omega$; f is frequency and ω is wavelength) and a cat's head size, this difference in time (Δt) varies from 0 to 400 μs for cats. The auditory system detects the Δt of sounds with $f < 2$ kHz and uses this Δt to localize sounds in the horizontal plane.

(C) A pure tone sound of 350 Hz elicits spikes in the cat auditory nerve. The time of the sound stimulus is shown, as well as timing of the spikes for 200 repetitions of the stimulus. Note that the spikes occur in a periodic way that follows the stimulus period. The spike timing is thus phase locked to the sound stimulus, and the timing of the spikes can be used to determine the frequency of the sound. But note that spikes do not occur for every cycle of the sound stimulus and the precision and fidelity of the spikes is degraded toward the end of the stimulus. On top of the auditory nerve data, recordings from an SBC axon are shown for a 340 Hz sound stimulus. These display an even better phase locking than auditory nerve spikes. Furthermore, spikes are elicited at almost every cycle of the sound stimulus and the precision of the timing is well preserved during the stimulus. Spikes in the SBC axon are thus highly synchronous and display more precision and endurance than spikes in the auditory nerve (modified from Joris et al., 1998).

(D) Recordings of spikes in the cat MSO principal cells. The two right panels show monaural responses elicited by stimulation of just the CONTRA or IPSI ear with a sound of 1 kHz. Spikes are phase locked to a particular phase of the sound stimulus and the Δt between the two peaks in monaural evoked firing rate is 140 μs. The left panel shows the firing rates when the same 1 kHz sound is heard by the two ears (binaural responses). Note that the central firing peak occurs near to 140 μs when both the CONTRA and IPSI excitatory signals coincide. This central peak determines the best delay (or best ITD, interaural time difference). The worst delay or ITD occurs at the red asterisk when firing rates go to zero. The blue rectangle shows the region where the peak ITD and maximum slope ITD occur. The green asterisks indicate secondary peaks in ITD that occur when a pure tone is used as a stimulus. If a more natural broadband sound (with several frequencies) is used as a stimulus, the MSO cell response shows an enhanced central peak because sounds of different frequencies still have a best delay near 140 μs. However, the secondary peaks are reduced with broadband sound stimuli. This explains why more natural broadband sounds can be better localized than artificial pure tone sounds (modified from Yin and Chan, 1990).

convergent input from the two ears, and fire maximally when the external delay (the time between the sound arriving at both ears; the ITD; Figure 1B) is exactly compensated by an internal delay that is due to differences in the lengths of axons that converge onto the coincidence detector neuron (Figure 1A). The bushy cell inputs to the MSO phase lock to low-frequency sounds, and MSO neurons fire maximally to coincident input (Figure 1D; Yin and Chan, 1990). They are sensitive

to positive ITDs, which means that they fire best to sounds that are on the contralateral side. This provides evidence for internal delay lines as it takes longer for the signal to travel from the contralateral ear compared to the ipsilateral ear.

While in birds there is both neurophysiological and anatomical support for the Jeffress model (Burger et al., 2011), it is more controversial in mammals. The controversies revolve around the origin of internal delays and the role of inhibition in shaping ITD tuning (Grothe et al., 2010). In contrast to the bird nucleus laminaris (NL; Burger et al., 2011), MSO neurons receive feedforward inhibitory input from the medial nucleus of the trapezoid body (MNTB) and the lateral nucleus of the trapezoid body (LNTB; Figure 1A; Chirila et al., 2007). How these inputs interact to shape sensitivity to ITDs in MSO neurons is not entirely clear. Blocking glycinergic inhibition bilaterally in vivo by iontophoretic application of strychnine broadens ITD tuning and shifts peak tuning toward 0 μs (Pecka et al., 2008). Thus, in mammals, glycinergic inhibition may function to actively shift the ITD selectivity of MSO neurons to preferentially respond to stimuli that lead in the contralateral ear. However, the elegant study by van der Heijden et al. (2013) provides compelling new evidence that ITD tuning in MSO neurons is determined by two simple features: the linear summation of the excitatory inputs from both ears and the nonlinear dependence of spike probability on the size of the EPSPs. Using in vivo whole-cell and juxtacellular recordings, they found no evidence of inhibition in the MSO neurons they recorded during presentation of pure tone binaural sounds. The authors suggest that the glycinergic input to MSO neurons may improve the dynamic range of the neurons as has been suggested in the NL in birds (Yamada et al., 2013) and in the SBCs (Kuenzel et al., 2011). It is also possible that inhibition plays a role in the localization of more natural broadband sounds composed of many frequencies (such as vocalizations) and for the cocktail party effect (suppression of sounds in noisy environments).

Clearly, the question of the in vivo role of inhibition in the MSO has not been fully answered. The second study in this issue (Roberts et al., 2013) provides new insight into the role that inhibition may play in the MSO. Roberts and colleagues developed a new thick slice preparation that includes the whole macrocircuit shown in Figure 1A, except for the cochlea. They were thus able to stimulate the auditory nerve and obtain IPSP and EPSP recordings from the MSO cells. This is the first time that IPSPs evoked by auditory nerve stimulation have been obtained from MSO neurons in brain slices. Surprisingly, they found that stimulating the inhibitory inputs from the LNTB and MNTB caused IPSPs in MSO neurons 300–400 μs prior to excitation, even though these pathways involve an extra synapse. They suggest that all the inhibitory sources of input to the MSO provide feed-forward inhibition that restricts the MSO neuron from firing except when the binaural excitatory inputs provide the largest, most synchronous EPSPs. In contrast to the in vivo experiments that blocked inhibition (Pecka et al., 2008), Roberts et al. (2013) did not find that the presence of inhibition shifted the location of the ITD function. Furthermore, both studies in this issue provide a case study of how to achieve linear synaptic integration using cellular mechanisms, like inhibitory synaptic conductances and potassium channel gating, that are individually nonlinear.

What are the biophysical mechanisms that allow coincidence detection à la Jeffress to occur? In the barn owls, recent tour de force in vivo recordings have shown that NL (the bird analog of the MSO) neurons have remarkable properties: (1) a very low input resistance and a passive soma that is devoid of Na^+ channels, (2) insanely fast EPSCs (half-width of 100 μs; perhaps due to higher bird-brain temperatures of 40°C–41°C), and (3) hundreds of phase-locked synaptic inputs from the contra and ipsilateral afferent axons (analogs of the SBC axons shown in Figure 1A; Funabiki et al., 2011). This allows the bird's NL neurons to function as leaky coincidence detectors that produce phase-locked spikes to sound frequencies of up to 8 kHz (Köppl, 2012). In mammals, phase locking can occur only for frequencies < 2–3 kHz. Like NL neurons, MSO neurons are very leaky (input resistance of 5–10 MΩ) and have small spikes (about 10–30 mV in amplitude), but unlike NL neurons they receive surprisingly few excitatory inputs from SBC axons (2–4 large excitatory fibers per dendrite) and do not appear to have ultrafast EPSCs (Couchman et al., 2010). The role of inhibition in these two circuits is also very different (see Roberts et al., 2013). Thus, the biophysical mechanisms for coding low frequency sounds appear to be very different in birds and small-headed mammals. Given that the tympanic ear evolved independently in frogs, birds, and mammals, these differences may not be too surprising (Grothe et al., 2010). Apart from these differences, a common mechanism has emerged from studies of different species: leaky coincidence detectors integrate excitatory signals from specialized synapses to produce well-timed spikes that encode the horizontal location of sound sources with amazing accuracy.

REFERENCES

Ashida, G., and Carr, C.E. (2011). Curr. Opin. Neurobiol. *21*, 745–751.

Burger, R.M., Fukui, I., Ohmori, H., and Rubel, E.W. (2011). J. Neurophysiol. *106*, 4–14.

Chirila, F.V., Rowland, K.C., Thompson, J.M., and Spirou, G.A. (2007). J. Physiol. *584*, 167–190.

Couchman, K., Grothe, B., and Felmy, F. (2010). J. Neurosci. *30*, 17111–17121.

Funabiki, K., Ashida, G., and Konishi, M. (2011). J. Neurosci. *31*, 15245–15256.

Grothe, B., Pecka, M., and McAlpine, D. (2010). Physiol. Rev. *90*, 983–1012.

Heffner, R.S., and Heffner, H.E. (1988). Behav. Neurosci. *102*, 422–428.

Joris, P.X., Smith, P.H., and Yin, T.C. (1998). Neuron *21*, 1235–1238.

Köppl, C. (2012). Curr. Biol. *22*, R56–R58.

Kuenzel, T., Borst, J.G.G., and van der Heijden, M. (2011). J. Neurosci. *31*, 4260–4273.

Payne, R.S. (1971). J. Exp. Biol. *54*, 535–573.

Pecka, M., Brand, A., Behrend, O., and Grothe, B. (2008). J. Neurosci. *28*, 6914–6925.

Roberts, M.T., Seeman, S.C., and Golding, N.L. (2013). Neuron *78*, this issue, 923–935.

van der Heijden, M., Lorteije, J.A.M., Plauška, A., Roberts, M.T., Golding, N.L., and Borst, J.G.G. (2013). Neuron *78*, this issue, 936–948.

Yamada, R., Okuda, H., Kuba, H., Nishino, E., Ishii, T.M., and Ohmori, H. (2013). J. Neurosci. *33*, 3927–3938.

Yin, T.C.T., and Chan, J.C.K. (1990). J. Neurophysiol. *64*, 465–488.